Biochimica et Biophysica Acta 1778 (2008) 2298–2307

Contents lists available at ScienceDirect

Biochimica et Biophysica Acta

journal homepage: www.elsevier.com/locate/bbamem

Micelle formation in the presence of photosystem I

Frank Müh [a,b,*], Athina Zouni [b]

[a] Institut für Chemie und Biochemie (Kristallographie), Freie Universität Berlin, Fabeckstrasse 36a, D-14195 Berlin, Germany
[b] Institut für Chemie/Max-Volmer-Laboratorium für Biophysikalische Chemie, Technische Universität Berlin, Strasse des 17. Juni 135, D-10623 Berlin, Germany

ARTICLE INFO

Article history:
Received 20 March 2008
Received in revised form 26 May 2008
Accepted 29 May 2008
Available online 13 June 2008

Keywords:
Crystallisation
Detergent
Fluorescence
Membrane protein
Pyrene

ABSTRACT

The correlation between membrane protein solubilisation and detergent aggregation in aqueous solution is studied for a series of *n*-alkyl-β-D-maltosides (C_xG_2 with x=10, 11, 12 being the number of carbon atoms in the alkyl chain) using the trimeric photosystem I core complex (PSIcc) of oxygenic photosynthesis from *Thermosynechococcus elongatus* as model protein. While protein solubilisation is monitored via the turbidity of the solution, the aggregation behavior of the detergent is probed via the fluorescence spectrum of the polycyclic aromatic hydrocarbon pyrene. In addition, changes of the fluorescence spectrum of PSIcc in response to formation of the detergent belt surrounding its hydrophobic surface are investigated. Solubilisation of PSIcc and aggregation of detergent into micelles or belts are found to be strictly correlated. Both processes are complete at the critical solubilisation concentration (CSC) of the detergent, at which the belts are formed. The CSC depends on the concentration of the membrane protein, [prot], and is related to the critical micelle concentration (CMC) by the empirical law $\ln(CSC/CMC)=\tilde{n}_0$ [prot], where the constant $\tilde{n}_0$ = (2.0±0.3) μM^{-1} is independent of the alkyl chain length x. Formation of protein-free micelles below the CSC is not observed even for x=10, where a significant excess of detergent is present at the CSC. This finding indicates an influence of PSIcc on micelle formation that is independent of the binding of detergent to the hydrophobic protein surface. The role of the CSC in the optimisation of membrane protein crystallisation is discussed.

© 2008 Elsevier B.V. All rights reserved.

1. Introduction

Fundamental processes such as photosynthesis or respiration are based on membrane-spanning multi-subunit protein complexes, which retain their activity after isolation from the cell and thus can be studied *in vitro*. A typical example is the trimeric photosystem I core complex (PSIcc) of the cyanobacterium *Thermosynechococcus elongatus*, a light-driven oxidoreductase that catalyses the reduction of ferredoxin and the oxidation of cytochrome c_6 or plastocyanin in oxygenic photosynthesis [1,2]. Significant progress in understanding the function of PSIcc was made due to the elucidation of its three-dimensional structure by X-ray crystallography [3] revealing 127 cofactors (including 96 chlorophyll *a* (Chl*a*) molecules) bound to 12 different protein subunits per PSIcc-monomer. However, compared to soluble proteins, the structural biology of membrane proteins is complicated by the use of detergents to keep these proteins soluble in aqueous solution [4,5].

Detergents are amphiphilic molecules that consist of a hydrophilic headgroup (e.g., a sugar molecule [6]) and a hydrophobic tail (usually an *n*-alkyl chain) [7–10]. In aqueous solution, they form globular aggregates, called micelles, above a certain concentration (*critical micelle concentration*, CMC) to shield their hydrophobic parts from the aqueous phase [11]. By binding with their tails to the hydrophobic surface of the membrane protein, detergents form a belt around the protein [12–17] and render the whole complex water soluble.

Protein crystallisation is induced by tuning protein–protein interactions through the addition of precipitating agents such as salts or polymers to promote the ordered assembly of protein particles into crystals in favour of amorphous precipitation. One measure of these interactions is the osmotic second virial coefficient [18], which has been found to be in a certain range under crystallisation conditions of soluble proteins, defining the so-called "crystallisation slot" [19]. Dynamic light scattering experiments revealed a correlation between crystallisation conditions and the so-called diffusion-limited cluster aggregation regime, which is characterised by an inter-particle potential that exhibits a small repulsive barrier $E_B<kT$ to aggregation [20].

In the case of membrane proteins, the influence of the detergent on the protein–protein interactions and the concomitant crystallisation behavior is still not well understood. The influence of precipitating agents on the micelles under crystallisation conditions, albeit in the

Abbreviations: bRC, bacterial reaction centre; Chl*a*, chlorophyll *a*; CMC, critical micelle concentration; CSC, critical solubilisation concentration; C_xG_2, *n*-alkyl-β-D-maltoside with *x* carbon atoms in the *n*-alkyl chain; PEG, polyethylene glycol; PSIcc, trimeric photosystem I core complex; PSIIcc, photosystem II core complex

* Corresponding author.
E-mail address: mueh@chemie.fu-berlin.de (F. Müh).

0005-2736/$ – see front matter © 2008 Elsevier B.V. All rights reserved.
doi:10.1016/j.bbamem.2008.05.016

absence of protein, has been investigated by small-angle neutron scattering [21]. The data indicate that membrane protein crystallisation is promoted under conditions, where the micelles have a low number density and are small, spherical, and noninteracting. The latter point was supported by similar studies on samples containing bacterial reaction centres (bRCs) as model proteins [22] indicating that bRC-monomers most likely serve as the crystal growth unit. However, monodispersity seems to be no strict requirement for the crystallisation of other proteins such as lysozyme (soluble) or the photosystem II core complex (PSIIcc) [23,24], exhibiting reversible aggregation at higher concentrations [20,25]. Another criterion proposed for crystallisation of bRC is the size of the detergent belt as indicated by the apparent radius of gyration R_g of the detergent-protein complex, which should lie in a certain range, defining an "R_g slot" [26].

On the basis of the foregoing, we may ask the following questions: What is the possible influence of the membrane protein itself on the aggregation behavior and micelle formation of the detergent? At which total detergent concentrations are the detergent belts and possibly additional free (i.e., protein-free) micelles formed? What is the influence of the free micelles on membrane protein crystallisation? What is the optimal detergent-protein ratio for crystallisation and its influence on the size of the detergent belt? How do the precipitating agents affect the various particle-particle interactions (i.e., protein–protein, belt–belt, belt–micelle etc.)?

The solubilisation of small hydrophobic molecules by detergents is strictly correlated with micelle formation [27–32]. The same is usually assumed to be true for the solubilisation of membrane proteins. However, neither has this assertion, to our knowledge, been explicitly studied by experiment, nor is it self-evident from a theoretical point of view. The detergent belt is a distinct type of aggregate, having different spatial extension and geometry and containing a larger number of detergent molecules than an ordinary micelle. Since the formation of detergent aggregates depends crucially on their structural characteristics [33–35], it is not clear *à priori* that the belts are formed at the same total concentration of detergent as the micelles.

Experimental studies of the bRC [36–38] as well as of PSIcc and PSIIcc [39] have shown that a minimal detergent concentration (*critical solubilisation concentration*, CSC) is required to solubilise a membrane protein. The CSC is higher than the CMC of pure detergent solutions and depends on the protein concentration. In the limit of small protein concentrations, [prot], this dependence is essentially linear and can be described by the simple empirical law

$$\mathrm{CSC} = \mathrm{CMC} + n_0[\mathrm{prot}], \quad (1)$$

where n_0 is the number of detergent molecules per protein complex that must be present in the solution in excess of the CMC to ensure solubilisation of the protein. There are three possible mechanisms, which, in principle, can explain such a behavior: 1. Micelles are formed at the CMC, but n_0 additional detergent molecules per protein complex are required to form the detergent belts. 2. Micelles and belts are formed simultaneously at the CSC. 3. Detergent belts are formed at the CSC, but the formation of free micelles occurs at even higher detergent concentrations.

One could argue that the binding of detergent molecules to the hydrophobic parts of the protein surface effectively removes detergent from the bulk phase and in this way shifts the micelle formation to higher total detergent concentrations. By analogy with other detergent-binding agents such as cyclodextrins [40–42], one could then relate the constant n_0 to the binding stoichiometry, i.e., simply assert that $n_0 = b$, where b is the average number of detergent molecules in the belt. This interpretation rejects the first of the three mechanisms outlined above and, in fact, has been used in earlier studies [36–39]. However, the problem is more complex, since n_0 scales with the CMC and for detergents with a high CMC is significantly larger than the number of detergent molecules that are likely to be bound to the protein. In these cases, it is not evident, which of the three mechanisms is true, and the question arises, why so many detergent molecules above the CMC are necessary to keep the protein in solution.

This problem motivated us to investigate the aggregation behavior of *n*-alkyl maltosides (C_xG_2 with alkyl chain length x) in the presence of PSIcc as a model membrane protein by using a hydrophobic dye as independent probe. A small hydrophobic molecule can enter the interior of the micelles, so that the solubility of the compound in the detergent phase is significantly increased compared to its solubility in pure water [7,43]. In many cases the change from the polar environment in water to the apolar environment within the micelle causes characteristic alterations of the spectroscopic properties of the molecule [27–32]. A prominent example is pyrene, which exhibits a richly structured fluorescence spectrum in the UV-VIS range (Fig. 1A). The intensities of the various vibronic bands are strongly dependent on the polarity of the solvent environment. In particular, the ratio of the first and third band (I_1/I_3-ratio) is decreased upon transferring the pyrene molecule from a pure water phase into micelles (Fig. 1B) [27,29–32]. Hence, the I_1/I_3-ratio can be used to monitor detergent aggregation during membrane protein solubilisation. Using this probe, we shall demonstrate that PSIcc influences the micelle formation of

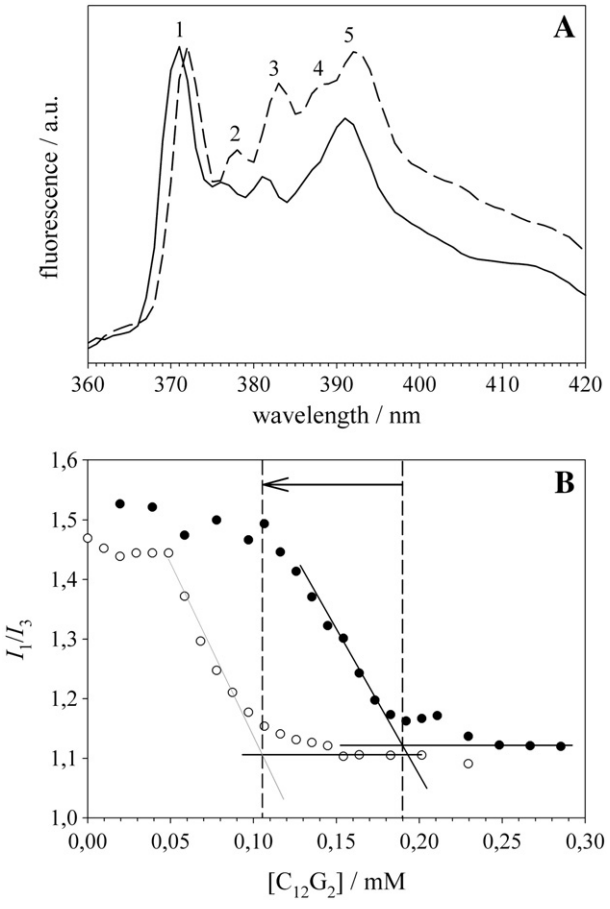

Fig. 1. (A) Fluorescence spectrum of pyrene in a solution containing 20 mM MES (pH 6.4) and either no detergent (solid) or $C_{12}G_2$ at a concentration above the CMC (dashed, ~0.3 mM). Excitation wavelength: 335 nm. The I_1/I_3-ratio is the intensity of the maximum of band 1 at ca. 370 nm versus the maximum of band 3 at ca. 380 nm. For better comparison, the spectra are normalized to band 1. (B) Dependence of the I_1/I_3-ratio on the concentration of the detergent $C_{12}G_2$ in either pure buffer (closed symbols) or in the presence of 0.5 M $MgSO_4$ (open symbols). The graphical extrapolation procedure to determine the CMC is shown for both titration curves. The arrow indicates the CMC shift due to the addition of electrolyte.

detergents in a way that goes beyond the mere binding to the hydrophobic protein surface and that the CSC rather than the CMC is the critical concentration for detergent aggregation under these conditions. In addition, we study the fluorescence of the protein-bound Chl*a* cofactors, which is itself sensitive to detergent–protein interaction [44–47] and thus serves as a direct probe for the formation of the detergent belt. The implications of the results for membrane protein crystallisation are discussed.

2. Materials and methods

Cells of *T. elongatus* were grown and PSIcc isolated and purified as described [39,48–50]. The protein was finally obtained in 20 mM MES (pH 6.4), 0.4 mM *n*-dodecyl-β-D-maltoside ($C_{12}G_2$), 50 mM $MgSO_4$. Detergents C_xG_2 (x=10–12) were purchased from Glycon (Luckenwalde, Germany). All spectroscopic experiments were performed with buffered solutions at room temperature. Detergent-depletion by BioBeads-treatment and turbidimetric titrations were done as in earlier work [39]. The pyrene stock solution for spectrofluorometry was prepared by suspending pyrene (Sigma) in water, followed by sonification and centrifugation. This resulted in a clear solution that was essentially free of pyrene aggregates as judged from the absence of excimer fluorescence [30]. The pyrene concentration used in the titration experiments was below $5\cdot10^{-7}$ M. Protein concentrations were determined by using the extinction coefficient of trimeric PSIcc, ε_{632}=14 μM^{-1} cm^{-1}, determined previously [39].

3. Results

3.1. Buffer and electrolyte effects on the CMC

Since the protein solutions in biochemical work usually contain buffer at a specific pH, and in the case of PSIcc, addition of electrolyte is necessary to solubilise the protein, we first investigated the influence of these ingredients on micelle formation. The detergents under study were *n*-alkyl-β-D-maltosides (C_xG_2) with alkyl chain lengths of x=10 (*n*-decyl), 11 (*n*-undecyl), and 12 (*n*-dodecyl). Typical fluorescence spectra of pyrene before and after micelle formation of $C_{12}G_2$ are shown in Fig. 1A and the corresponding titration curves in Fig. 1B. Upon increasing the detergent concentration step by step, the initially high I_1/I_3-ratio is significantly decreased in a certain concentration range and remains low at higher concentrations. The intensity of band 3 relative to that of band 1 is known to be an indicator of solvent polarity [27,30]. Therefore, the steep decrease of the I_1/I_3-ratio is interpreted as evidence for the formation of hydrophobic compartments in the solution originating from detergent aggregation into micelles. The decrease of the fluorescence ratio is not sudden, but occurs over a detergent concentration interval of about 0.1 mM for $C_{12}G_2$. Often we observe a slight decrease of I_1/I_3 below that interval, which could indicate some detergent-pyrene interaction at very low detergent concentrations. Above that interval, the titration curves asymptotically approach the final I_1/I_3-ratio, so that a graphical extrapolation procedure is used to determine the CMC as indicated in Fig. 1B. The CMC values obtained in this way typically show variations on the order of 10–15%. Hence, several titrations (usually at least five) are performed for each set of conditions and the results averaged.

We investigated micelle formation of $C_{12}G_2$ at different pH-values between 5.0 and 9.0 using either 20 mM MES or 20 mM Tris. The same CMC of (0.19±0.02) mM was found in all cases. This value is in good agreement with literature data for pure aqueous solutions [28,29]. Therefore, we consider the CMC of this class of detergents as insensitive to the buffer conditions used in our experiments.

In contrast, a pronounced decrease of the CMC of $C_{12}G_2$ is caused by the addition of $MgSO_4$, a common electrolyte used in the biochemical preparation of PSIcc. The CMC is decreased significantly from 0.19 to 0.11 mM upon increasing the $MgSO_4$-concentration to 0.5 M (Fig. 1B). Note that the detergent concentration interval, in which the major changes of the I_1/I_3-ratio occur, is narrower at higher ionic strength.

The CMC is known to depend exponentially on the alkyl chain length x for the same detergent headgroup. We observed values of 1.8 mM (x=10), 0.49 mM (x=11), and 0.19 mM (x=12) for the alkyl maltosides resulting in the relationship

$$\ln(CMC_0/mM) = 12 - 1.14x, \quad (2)$$

where CMC_0 is the CMC at zero ionic strength (buffered solutions). In all cases studied, the addition of $MgSO_4$ causes a decrease of the CMC amounting to ~50% at 0.5 M $MgSO_4$. The electrolyte effect can be described by the empirical relationship

$$\ln(CMC/CMC_0) = -1.14\,[MgSO_4]/M. \quad (3)$$

3.2. Correlation of PSIcc solubilisation with I_1/I_3-ratio

A typical resolubilisation experiment, in which detergent ($C_{12}G_2$) is added stepwise to a suspension of detergent-depleted PSIcc in the presence of small amounts of pyrene, is shown in Fig. 2. In each step, we monitored both the turbidity of the suspension/solution via the extinction at 550 nm, E_{550}, and the I_1/I_3-ratio of pyrene. The dependence of E_{550} on the concentration of added detergent exhibits the same behavior as observed earlier for bRC [36–38] as well as PSIcc and PSIIcc [39]. The high extinction at low detergent concentrations is caused by protein aggregates, while the steep decrease of E_{550} close to the CSC indicates the detergent-induced dissociation of these aggregates. The CSC is determined by a graphical extrapolation procedure as demonstrated in Fig. 2.

Similar to the case of protein-free solutions, the I_1/I_3-ratio in the presence of PSIcc is initially high and then decreases within a certain interval of detergent concentrations. We found no significant influence of PSIcc on the emission spectra of pyrene, apart from a decreased signal-to-noise ratio at lower detergent concentrations. The latter apparently originates from the scattering of emitted light by the protein aggregates and correspondingly depends on the protein concentration. This effect limits the PSIcc concentrations, at which the I_1/I_3-ratio can be determined faithfully, to a maximum of about 0.25 μM.

The decrease of the I_1/I_3-ratio is clearly correlated with the decrease of E_{550}. The graphical extrapolation procedure can be applied to both curves and yields the same value for the CSC within the error

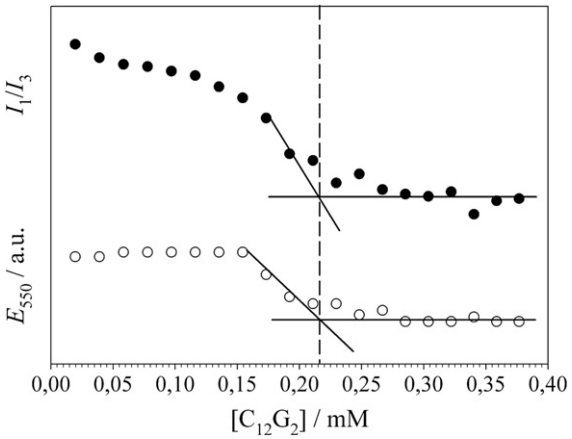

Fig. 2. Titration of a suspension of 0.06 μM detergent-depleted PSIcc in 20 mM MES (pH 6.4), 50 mM $MgSO_4$ with $C_{12}G_2$ in the presence of ~0.3 μM pyrene. Shown are the I_1/I_3-ratio of pyrene fluorescence and the turbidity of the suspension as measured via the extinction at 550 nm (upscaled tenfold for better comparison). The dashed line indicates the CSC.

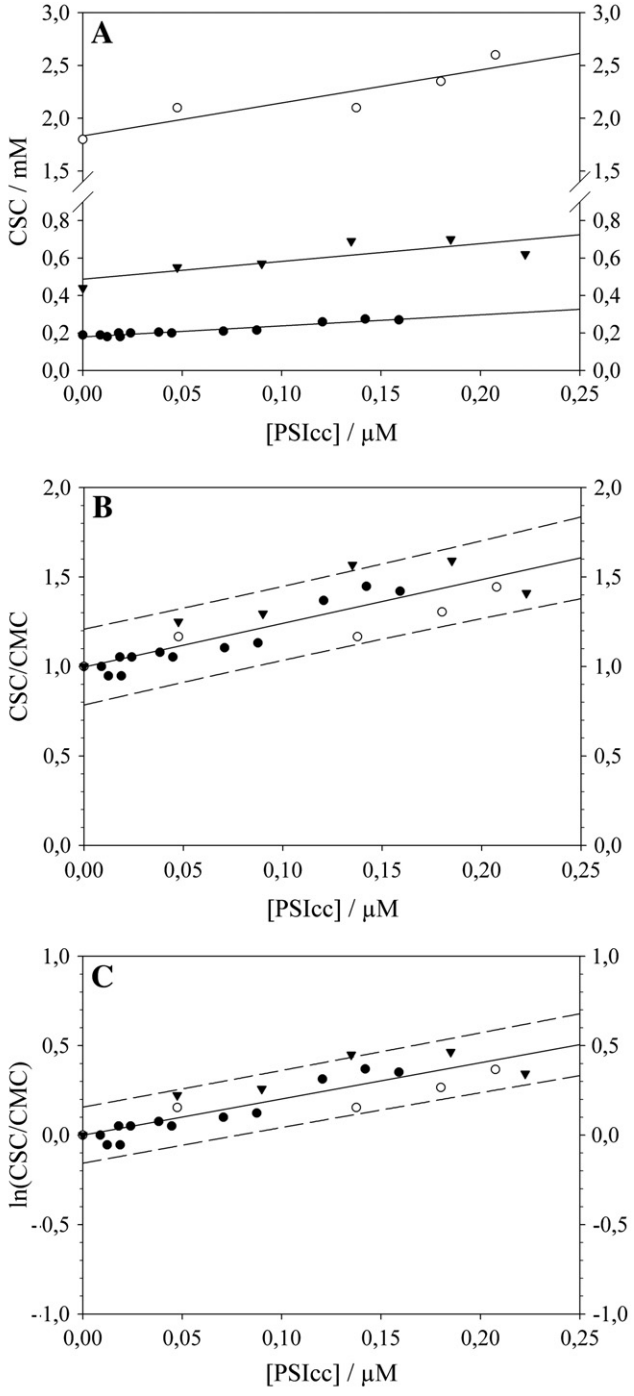

Fig. 3. (A) Dependence of the CSC of $C_{10}G_2$ (○), $C_{11}G_2$ (▼), $C_{12}G_2$ (●) on the concentration of PSIcc in 20 mM MES (pH 6.4), 50 mM $MgSO_4$. (B) Same as in A, but with the CSC at a given PSIcc concentration rescaled by division through the CMC at zero PSIcc concentration. The solid line follows from linear regression (Eq. (4)) involving all data points and has slope (2.4 ± 0.3) μM^{-1} and intercept 1. The dashed lines indicate the 95% prediction interval of CSC/CMC as a function of protein concentration. (C) Same as in B, but with the ordinate representing ln(CSC/CMC). The solid line follows from linear regression (Eq.(5)) involving all data points and has slope (2.0 ± 0.3) μM^{-1}. The dashed lines indicate the 95% prediction interval of ln(CSC/CMC) as a function of protein concentration.

limits. Thus, the I_1/I_3-ratio provides an alternative probe of the CSC. Interestingly, the major changes of both observables, I_1/I_3 and E_{550}, occur in the same detergent concentration interval. Membrane protein solubilisation is, therefore, associated with the formation of hydrophobic compartments in the solution as expected. However, protein solubilisation and detergent aggregation are both not complete at the CMC, but at the higher CSC.

The analysis of the I_1/I_3-ratio reveals an essentially linear dependence of the CSC on the PSIcc concentration (Fig. 3A) in accordance with Eq. (1) and in line with the turbidimetric experiments. There is a pronounced dependence of the slope n_0 on the alkyl chain length x (Table 1) as observed earlier for other types of detergents [36–38]. This dependence is exponential and resembles that of the CMC so that for all detergents studied

$$\mathrm{CSC/CMC} = 1 + \bar{n}_0[\mathrm{prot}] \quad (4)$$

with $\bar{n}_0 = n_0/\mathrm{CMC} = (2.4 \pm 0.3)\ \mu M^{-1}$. The number of detergent molecules, that have to be present in the solution in excess of the CMC to ensure protein solubilisation, can be estimated from $n_0 = \bar{n}_0 \cdot \mathrm{CMC}$ as shown in Table 1. The values differ from those obtained from a fit to Eq. (1), but are on the same order of magnitude. The two different ways of analysing the data give an impression of the uncertainty of the n_0 values.

We note that Eq. (4) can be regarded as a linear approximation (valid for CSC/CMC ≤ 2) of the logarithmic form

$$\ln(\mathrm{CSC/CMC}) = \bar{n}_0[\mathrm{prot}], \quad (5)$$

which is similar to Eq. (3) describing the electrolyte effect. A fit of the experimental data to Eq.(5) yields $\bar{n}_0 = (2.0 \pm 0.3)\ \mu M^{-1}$ (Fig. 3C, Table 1).

3.3. Detergent effects on PSIcc fluorescence

After detergent depletion by BioBeads-treatment and suspension in buffer, PSIcc shows a characteristic emission spectrum in the Chl*a* Q_Y region around 700 nm when excited at 435 nm (Fig. 4A). The spectrum exhibits a main emission maximum at about 710 nm and a side band to higher energies at about 680 nm. This particular spectrum is expected to represent the native form of PSIcc that would be observed for PSIcc embedded in the photosynthetic membrane [44,45]. Addition of detergent causes significant alterations of the spectrum. The emission around 680 nm increases with increasing detergent concentration,

Table 1
Parameters describing detergent aggregation in the absence and presence of PSIcc

Detergent[a]	$C_{10}G_2$	$C_{11}G_2$	$C_{12}G_2$
CMC/mM (exp.)[b]	1.8±0.1	0.49±0.05	0.180±0.004
n_0[b,c]	3100±800	950±40	590±60
$\bar{n}_0 \cdot$ CMC (linear)[c,d]	4300±800	1180±270	430±70
(logarithmic)[c,e]	3600±800	980±250	360±70
r/nm[f]	2.40	2.55	2.70
V_{mol}/(nm^3)[g]	0.637	0.664	0.691
b (area)[h]	900–1100	970–1200	1040–1250
(volume)[i]	980	1070	1160
m[j]	81	105	125
$\Delta\mu_{mic}/kT$[k]	−16.8	−18.3	−19.8
CMC/mM (calc.)[l]	2.78	0.63	0.15

[a] 20 mM MES (pH 6.4), 50 mM $MgSO_4$.
[b] From fit to Eq. (1). The given errors are the standard deviations obtained from linear regression.
[c] Concentration of PSIcc-trimer given in mM.
[d] From fit to Eq. (4). Error calculated from the errors of $\bar{n}_0$ and CMC.
[e] From fit to Eq. (5). Error calculated from the errors of $\bar{n}_0$ and CMC.
[f] Extended length of the detergent molecule.
[g] Calculated from $V_{mol}(C_{12}G_2) - (12-x)\ V(CH_2)$ with $V_{mol}(C_{12}G_2) = 0.691$ nm^3 [63] and $V(CH_2) = 0.0269$ nm^3 [35].
[h] Estimated number of detergent molecules in the belt from $b \approx A_{HT}/A_M$, $A_M = 0.5$–0.6 nm^2, A_{HT} from Eq. (6), and $R = 10$ nm inferred from the crystal structure [3].
[i] Estimated number of detergent molecules in the belt from $b \approx V_{HT}/V_{mol}$, V_{HT} from Eq. (7), and $R = 10$ nm inferred from the crystal structure [3].
[j] Aggregation number of free micelles, from Ref. [65].
[k] From Eq. (10).
[l] From Eq. (11).

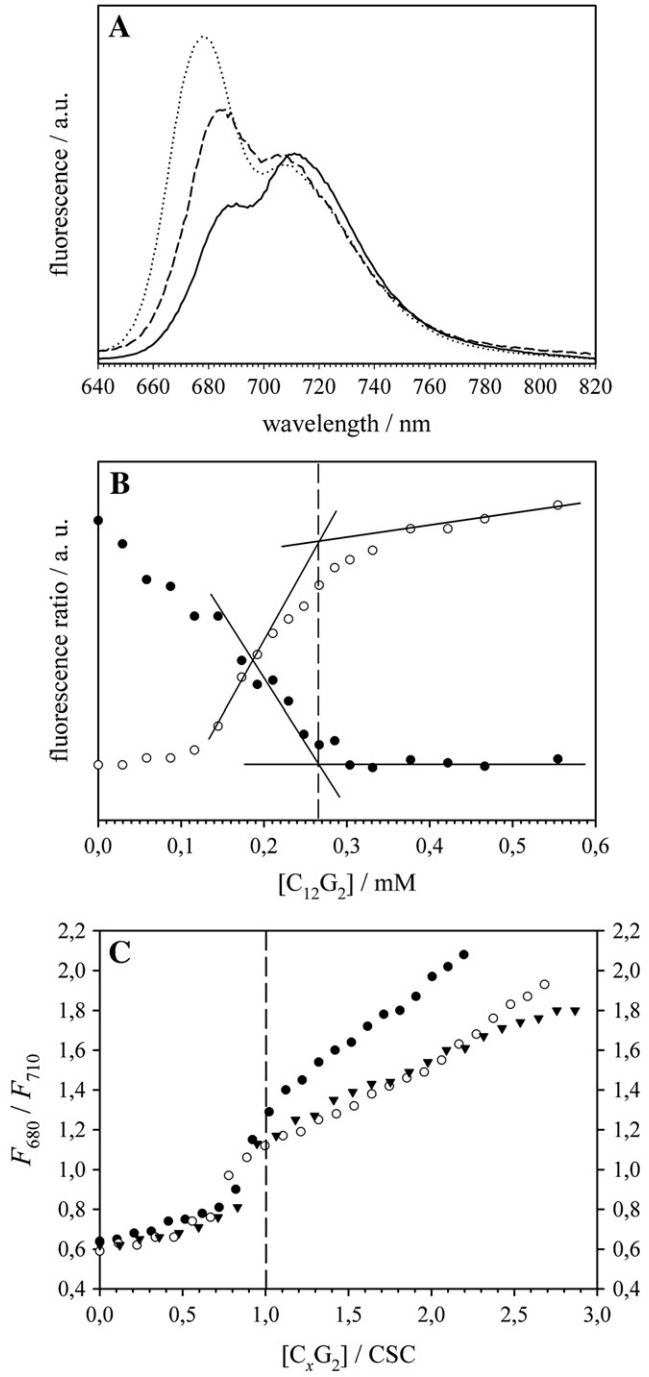

Fig. 4. (A) Fluorescence spectrum of detergent-depleted PSIcc before (solid) and after (dotted) addition of $C_{12}G_2$ at a concentration of 1.2 CSC. Excitation wavelength: 435 nm. The maxima of the emission peaks referred to as F_{680} and F_{710} are shifted from 687 and 711 nm to 676 and 707 nm, respectively. The dashed spectrum is obtained after dilution of the sample with detergent-free buffer to shift the detergent concentration below the CSC (upscaled for better comparison). (B) Titration of a suspension of 0.14 μM detergent-depleted PSIcc in 20 mM MES (pH 6.4), 50 mM $MgSO_4$ with $C_{12}G_2$ in the presence of ~0.3 μM pyrene. Shown are the I_1/I_3-ratio of pyrene fluorescence (closed symbols) and the F_{680}/F_{710} ratio of PSIcc (open symbols). The fluorescence ratios are rescaled for better comparison. The dashed line indicates the CSC. (C) Dependence of the F_{680}/F_{710} ratio of PSIcc on the concentration of $C_{10}G_2$ (○), $C_{11}G_2$ (▼), $C_{12}G_2$ (●) rescaled by division through the CSC. The dashed line indicates $[C_xG_2]$=CSC.

while the emission around 710 nm remains almost unchanged. This result is in agreement with earlier observations made on different types of PSIcc preparations [44–47]. The effect is partially reversible, i.e., dilution of the sample with detergent-free buffer to shift the detergent concentration below the CSC causes a decrease of the 680 nm band relative to the 710 nm band (Fig. 4A).

In the following we shall denote the intensity of the emission maximum around 680 nm with F_{680} and that around 710 nm with F_{710}. Fig. 4B shows the explicit dependence of the F_{680}/F_{710} ratio of PSIcc on the concentration of $C_{12}G_2$ together with the I_1/I_3-ratio of pyrene measured on the same sample. There is an obvious correlation between the two quantities. The F_{680}/F_{710} ratio increases only slightly at low detergent concentrations followed by a steep increase that coincides with the steepest decrease of the I_1/I_3-ratio. Above the CSC, F_{680}/F_{710} is not a constant, but approaches asymptotically an essentially linear dependence on the detergent concentration. These results show that in the particular case of PSIcc the protein-bound Chl*a* can be used as indicator to determine the CSC. The changes of the fluorescence spectrum of PSIcc are correlated with the formation of detergent aggregates and the solubilisation of the membrane protein, i.e., are caused by the formation of the detergent belt. Accordingly, the qualitative dependence of F_{680}/F_{710} on the detergent concentration is the same for all detergents studied. A quantitative coincidence of the various titration curves can be achieved, if the detergent concentration is rescaled by division through the CSC as demonstrated in Fig. 4C.

4. Discussion

4.1. What is the meaning of the changed fluorescence ratios?

In the present work, we have shown that the solubilisation of membrane proteins by detergents, i.e., the dissociation of protein aggregates, is correlated with the formation of hydrophobic compartments in the solution. Albeit not surprising, this result is not self-evident, because it was not known *à priori*, how the protein influences the detergent. By using the I_1/I_3-ratio of pyrene, we could demonstrate that the CSC is indeed the critical concentration for the formation of detergent aggregates in the presence of the membrane protein.

The I_1/I_3-ratio senses the polarity of the environment, but not the geometric characteristics of the hydrophobic compartments. Therefore, the method cannot distinguish between detergent belts and free micelles. Since the I_1/I_3-ratio is high in the presence of the membrane protein before addition of detergent, there are no indications for a preferential binding of pyrene to hydrophobic parts of the protein surface. Furthermore, the residence time of pyrene in a micelle is typically below 1 ms [8,9] so that it can be expected to rapidly exchange between micelles and belts. A low I_1/I_3-ratio thus indicates the presence of either belts or micelles or both, whereas a high I_1/I_3-ratio implies the absence of both types of aggregates. This means, in particular, that free micelles are not formed below the CSC, i.e., the first of the three mechanisms outlined in the Introduction can be dismissed.

The change of the F_{680}/F_{710} ratio of PSIcc due to addition of detergent is a well-known effect [44–47]. We have demonstrated that it is correlated with both the formation of detergent aggregates and protein solubilisation. This result allows to strictly identify the CSC with the critical concentration for the formation of the detergent belt. It remains open, however, whether free micelles are formed simultaneously or at higher detergent concentrations. A distinction between the second and third mechanism (cf. Introduction) requires other methods that allow to determine the sizes of the various detergent aggregates (e.g., small-angle neutron scattering [22,26] or fluorescence correlation spectroscopy [51]).

The molecular mechanism of the changed F_{680}/F_{710} ratio as well as its further increase above the CSC is not yet understood. The 680 nm fluorescence of PSIcc is frequently interpreted in terms of "uncoupled" Chl*a*, i.e., Chl*a* that lost their ability to transfer excitation energy to those Chl*a* emitting at 710 nm. This uncoupling could be due to either extraction of Chl*a* from the protein scaffold of PSIcc or a conformational change of the core antenna system. Although we cannot exclude

that the first possibility is responsible for at least part of the F_{680} fluorescence, we think that extraction of Chl*a* is unlikely for two reasons. First, alkyl maltosides are mild detergents in contrast to, e.g., Triton X-100 [52] or sulfobetaines [48]. The former are known to retain the high Chl*a*/RC ratio of PSIcc and, therefore, are used for protein isolation and purification [48,49]. We can assume that those Chl*a* seen in the crystal structure are tightly enough bound to the protein so that even extensive washing with $C_{12}G_2$ on an anion exchange column does not remove them. The same arguments hold for small Chl*a*-binding protein subunits of PSIcc that might be lost upon detergent treatment. Second, the effect is reversible. The residual F_{680} fluorescence observed after dilution of the sample below the CSC (Fig. 4A) can be traced back to incomplete detergent removal from the protein surface and is decreased by further dilution or BioBeads-treatment. We thus prefer the second explanation, a conformational change of the core antenna of PSIcc. A reversible detergent-induced conformational switch has been observed earlier in the case of bRC [38,53–59].

4.2. Is the slope n_0 really the number b of detergent molecules bound to the protein?

The effect of the membrane protein on detergent aggregation is characterised by the constant n_0 in Eq. (1). It corresponds to the number of detergent molecules per protein complex that must be present in the solution in excess of the CMC to ensure formation of the detergent belt. The interpretation of this quantity as the number of detergent molecules b in the belt is, however, questionable in view of its dependence on the alkyl chain length x of the detergent: The approximate shape of the detergent belt as indicated by X-ray crystallography [12,13,15,16] and molecular dynamics simulations [17] allows to estimate b on the basis of a simple geometric model. The membrane-spanning part of the PSIcc-trimer has an approximately cylindrical shape [3], so that we can regard the detergent belt as a half-torus as sketched in Fig. 5. This idealized geometry of the detergent belt is a simplification inasmuch a sphere or ellipsoid is an idealization of the real shape of a free micelle [11,17,60]. In such a model, the detergent headgroups (maltose moieties) are assumed to cover the outer surface of the half-torus (Fig. 5B), the area A_{HT} of which can be calculated from the major radius R of the cylinder occupied by the membrane protein and the minor radius r representing half of the thickness of the membrane [61]:

$$A_{HT} = 2\pi^2 rR + 4\pi r^2. \quad (6)$$

Note that the surface of the outer half of the torus is larger than half the surface of the full torus ($2\pi^2 rR$) by an amount corresponding to the surface of a sphere with minor radius r. The headgroup area A_M of the alkyl maltosides (representing the required space of the headgroup rather than its molecular size) is 0.5–0.6 nm^2 [60,62–64], while the crystal structure of PSIcc [3] suggests that R=10 nm. For the minor radius r we use the extended length of the detergent molecule as suggested by the work of Roth et al. [12,13]. The obtained values are in reasonable agreement with n_0 for $C_{11}G_2$ only, whereas $b<n_0$ for $C_{10}G_2$ and $b>n_0$ for $C_{12}G_2$ (Table 1).

A more precise estimate of b may be obtained from the ratio of the volume of the half-torus

$$V_{HT} = \pi^2 r^2 R + 4\pi r^3/3, \quad (7)$$

given by half the volume of the full torus ($\pi^2 r^2 R$) plus the volume of a sphere with minor radius r, and the molecular volume of the detergent

$$V_{mol} = V_M + (x-1)V(CH_2) + V(CH_3), \quad (8)$$

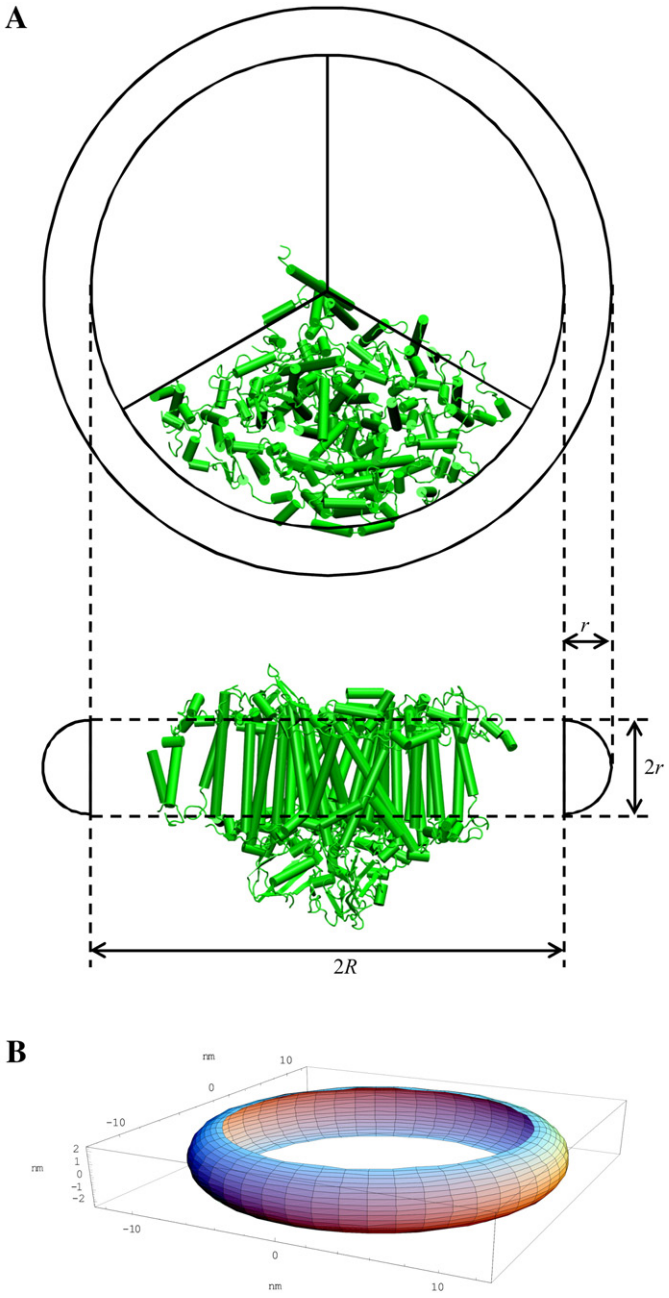

Fig. 5. Simple geometric model of the detergent belt surrounding PSIcc in aqueous solution. (A) Dimensions of PSIcc as inferred from the crystal structure [3] with R=10 nm. The radius r is the extended length of a detergent molecule (2.4–2.7 nm, Table 1). One PSIcc-monomer is shown as backbone cartoon in green. (B) Outer surface of the half-torus used as model for the detergent belt. The area of this surface is given by Eq. (6) and the volume of the half-torus by Eq. (7). Calculation of surface and volume and creation of the figure were performed by using *Mathematica* [61].

where V_M, $V(CH_2)$ and $V(CH_3)$ are the volumes of the maltose headgroup, the methylene unit and the methyl group, respectively. The numbers calculated in this way agree well with the estimates based on the area ratios (Table 1).

The simple geometric model predicts a slight increase of b with increasing x. This prediction is in line with experimental observations based on measurements of the apparent radius of gyration R_g or Stokes radius of detergent–protein complexes. Bamber et al. recently studied a mitochondrial ADP/ATP carrier solubilised with *n*-alkyl maltosides [65]. The numbers b=105 for $C_{10}G_2$, 130 for $C_{11}G_2$, and 156 for $C_{12}G_2$

$$\frac{ab}{m}\,\mathrm{D}_m + \mathrm{P}_a \overset{K_{\mathrm{mic}}}{\rightleftharpoons} ab\,\mathrm{D} + \mathrm{P}_a \overset{K_{\mathrm{belt}}}{\rightleftharpoons} a\,\mathrm{PD}_b$$

Scheme 1.

were found to follow the same trend as the aggregation numbers m of free micelles, being 81, 105, and 125, respectively. A comparison of the latter data with the estimated values of b suggests that in the case of PSIcc, $b \approx 10\,m$ (Table 1). Marone et al. investigated the bRC solubilised with n-alkyl glucosides and found a similar increase of R_g with x [26]. A preliminary study of PSIIcc using dynamical light scattering indicates that the effective radius of the detergent–PSIIcc complex is approximately the same in $C_{10}G_2$ and $C_{12}G_2$, i.e., at least not larger for $x=10$ than for $x=12$ (Zouni, A., unpublished data). These results are hard to reconcile with an exponential increase of b with decreasing x. We thus conclude that, in general, $n_0 \neq b$.

4.3. What are the implications for micelle formation?

To address the question of micelle formation in the presence of PSIcc, we shall consider a simple mass-action model as depicted in Scheme 1.

Here, D stands for a detergent monomer and P for a single protein complex (i.e., trimeric PSIcc). The numbers a, b, and m are the aggregation number of unsolubilised protein, detergent molecules in the belt and aggregation number of free micelles, respectively. Thus, D_m is a micelle and PD_b a solubilised protein complex. In the spirit of the mass-action (or closed association) model [8–10], polydispersity of aggregates is neglected so that a, b, and m represent the most probable aggregate sizes.

The equilibrium constant K_{mic} for micelle formation is related to the free energy change per detergent molecule $\Delta\mu^0_{\mathrm{mic}}$ for the transfer of the monomer D into the micelle by

$$K_{\mathrm{mic}} = \frac{X_{\mathrm{mic}}}{X_1^m} = \exp\left[-\frac{m\Delta\mu^0_{\mathrm{mic}}}{kT}\right], \tag{9}$$

where X_{mic} and X_1 are the mole fractions of micelles and monomers, respectively, and k is Boltzmann's constant. The quantity $\Delta\mu^0_{\mathrm{mic}}$ can be obtained from a molecular thermodynamic approach [34,35], where it is decomposed into several terms. The most important terms are those due to the hydrophobic effect [66–70] and the headgroup repulsion [35]. The former effect determines the free energy change of transferring the alkyl chain from water into a liquid hydrocarbon state representing the inner core of the micelle. The latter is mainly due to steric interaction between the headgroup moieties in the case of nonionic detergents, which is difficult to calculate accurately. We, therefore, consider here only the transfer term, which is responsible for the exponential dependence of the CMC on x. Using solubility data for hydrocarbon gases in water and considering the different behavior of methylene and methyl groups, one arrives at the following result [35]:

$$\Delta\mu^0_{\mathrm{mic}}/kT = -3.5 - 1.48(x-1) \tag{10}$$

with $kT = 25.7$ meV at room temperature ($T = 298$ K). As shown in Table 1, the order of magnitude of the CMC can be estimated well by

$$\ln X_{\mathrm{CMC}} = \Delta\mu^0_{\mathrm{mic}}/kT, \tag{11}$$

where $X_{\mathrm{CMC}} \approx X_1 = mX_{\mathrm{mic}}$ at the CMC is assumed and CMC = $X_{\mathrm{CMC}} \cdot 55.51$ mol L^{-1}. The deviations of the calculated from the measured CMC values reflect the neglect of headgroup repulsion and other terms, the computation of which is beyond the scope of the present work.

The equilibrium constant K_{belt} for the formation of a detergent belt in the presence of a protein aggregate P_a is given by

$$K_{\mathrm{belt}} = \frac{X^a_{\mathrm{belt}}}{X_1^{ab} X_{\mathrm{P}}} = \exp\left[-\frac{\Delta G^0_{\mathrm{sol}}}{kT}\right], \tag{12}$$

where X_{belt} and X_{P} are the mole fractions of belts (i.e., solubilised protein complexes) and protein aggregates, respectively. The free energy of solubilisation $\Delta G^0_{\mathrm{sol}}$ can be decomposed according to the thermodynamic cycle depicted schematically for $a = 2$ in Fig. 6:

$$\Delta G^0_{\mathrm{sol}} = \Delta G^0_{\mathrm{diss}} + \Delta G^0_{\mathrm{belt}} \tag{13}$$

into the sum of the free energy for aggregate dissociation $\Delta G^0_{\mathrm{diss}}$ and the free energy for assembly of the detergent belt from detergent monomers $\Delta G^0_{\mathrm{belt}}$. These two components in turn can be written

$$\Delta G^0_{\mathrm{diss}} = -a\Delta\mu^0_{\mathrm{ass}} \tag{14}$$

and

$$\Delta G^0_{\mathrm{belt}} = ab\eta\Delta\mu^0_{\mathrm{int}} + ab(1-\eta)\Delta\mu^0_{\mathrm{belt}}. \tag{15}$$

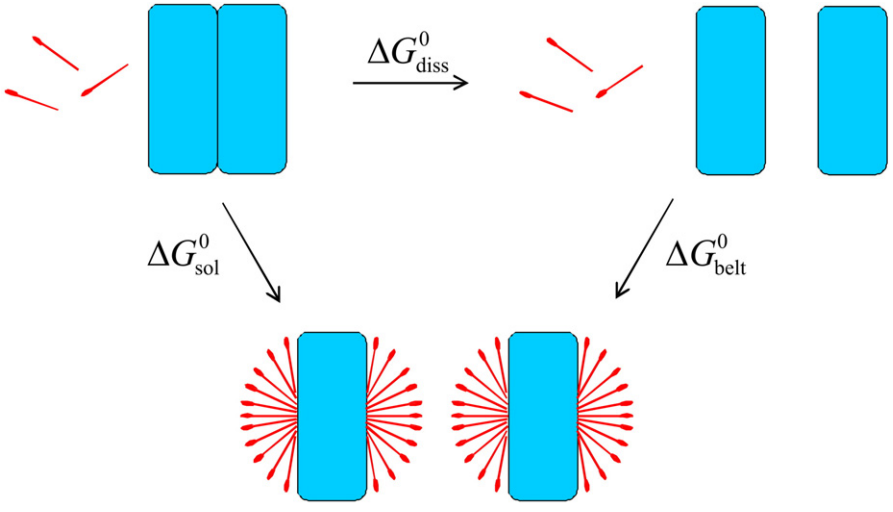

Fig. 6. Thermodynamic cycle relating the free energy change of membrane protein solubilisation $\Delta G^0_{\mathrm{sol}}$ to the free energy changes of protein aggregate dissociation $\Delta G^0_{\mathrm{diss}}$ and detergent belt assembly $\Delta G^0_{\mathrm{belt}}$.

Here, $\Delta\mu^0_{ass}$ is the free energy for association of the protein aggregate per single protein complex and $\Delta\mu^0_{belt}$ is correspondingly the free energy for formation of the detergent belt per detergent monomer comprising only contributions from detergent–detergent interactions. All detergent–protein interactions are contained in $\Delta\mu^0_{int}$, and η is the fraction of detergent molecules in the belt that are in direct contact with the protein. It is reasonable to assume that $\Delta\mu^0_{int}$ and $\Delta\mu^0_{belt}$ depend linearly on x as does $\Delta\mu^0_{mic}$ and that this dependence dominates ΔG^0_{sol}. In this way, we can understand, why the CSC lies in a similar range of absolute detergent concentration as does the CMC, a range that varies by an order of magnitude for the detergents studied.

To understand the apparent dependence of detergent aggregation on the protein concentration, we shall assess the concentration c of detergent not bound to the protein at the CSC. If we assume for simplicity that $b \approx 10^3$ for all detergents studied and that the protein is completely solubilised at the CSC, we have $c = \mathrm{CSC} - b\,[\mathrm{prot}]$, which at 0.25 μM PSIcc is 2.7, 0.56, and 0.05 mM for $C_{10}G_2$, $C_{11}G_2$, and $C_{12}G_2$, respectively. Thus, we have $c > \mathrm{CMC}$ for $x = 10$, $c \approx \mathrm{CMC}$ for $x = 11$, and $c < \mathrm{CMC}$ for $x = 12$. The fluorescence data indicate that detergent aggregation is not complete at the CMC<CSC in the presence of protein. Hence, the case $c > \mathrm{CMC}$ clearly demonstrates an influence of the protein on micelle formation. Note that for $x = 10$, there is a significant excess of "free" detergent with respect to protein-bound detergent present at the CSC. If the CMC would not be upshifted by the protein, detergent aggregation should be almost complete at 1.8 mM $C_{10}G_2$, which is not observed. We conclude that K_{mic} in the presence of protein is smaller than K_{mic} in the absence of protein. Since K_{mic} does not depend on the direct binding of detergent to the hydrophobic protein surface, this effect requires to postulate an influence of the membrane protein on the activity coefficients of detergent monomers (γ_1) and/or micelles (γ_{mic}):

$$\Delta G^{NI}_{mic} = m\Delta\mu^0_{mic} + kT \ln\left(\frac{\gamma_{mic}}{\gamma_1^m}\right), \tag{16}$$

where ΔG^{NI}_{mic} is the nonideal free energy change of micelle formation. The effect of electrolyte can be understood in a similar way, but whereas $\gamma_{mic} < \gamma_1^m$ for the electrolyte, $\gamma_{mic} > \gamma_1^m$ for the membrane protein. A qualitatively similar effect on micelle formation to be interpreted by $\gamma_{mic} > \gamma_1^m$ is observed for hydrophilic polymers such as polyethylene glycol (PEG) [21,29], which is expected to bind essentially no detergent at its surface. Indeed, we also found an increase of the CMC of $C_{12}G_2$ due to addition of PEG (Müh, F., and Zouni, A., unpublished data). However, the mechanism of this CMC upshift remains elusive.

4.4. What are the implications for membrane protein crystallisation?

Precipitating agents such as salts or polymers used in crystallisation experiments influence the solubility of detergents and thus shift the CMC. If we assume that the formation of the detergent belt is dominated by ΔG^0_{belt} in Eq. (15) and this quantity is affected by the precipitating agent similarly to ΔG^{NI}_{mic} as suggested above, we can expect the CSC to be shifted in the same direction as the CMC. Therefore, the concentration gradient of the precipitating agent in a typical crystallisation setup, e.g., the decreasing $MgSO_4$ concentration in the case of PSIcc [3,49] or the increasing PEG concentration in the case of PSIIcc [71–73], will not only change the protein-protein interactions, but also bring the system closer to the CSC without changing the overall detergent/protein ratio in the sample. Information about the dependence of $\tilde{n}_0$ on the concentration of the precipitating agent could therefore be important to optimise the crystallisation conditions.

By a similar analogy between micelles and belts we can expect the belts to slightly grow above the CSC as do the micelles above the CMC [74,75]. If this is true, the effective radius R_g of the detergent-protein complex will be minimal in a region right above the CSC. Thus, there should exist a "CSC slot" related to the "R_g slot" proposed by Marone et al. [26]. It is intriguing to speculate whether in the case of membrane proteins the main effect of the precipitating agent is to reduce R_g until the detergent–protein complex reaches a critical radius suitable for arrangement into the crystal lattice. This would be worth a further investigation.

The influence of free micelles on the crystallisation process depends on their interaction with the hydrophilic surfaces of the protein and detergent belts, which in turn is affected by the precipitating agent. It is probably difficult to find conditions, where protein–protein contacts are favoured, but not micelle–protein and micelle–micelle contacts. Since the latter contacts disturb the crystallisation, the number density of free micelles should be minimised. Even though we are not able to determine the concentration of free micelles in our experiments, we can reasonably assume that the micelle concentration will increase with increasing detergent concentration above the CSC. Hence, the "CSC slot" implies not only a minimised R_g, but also a minimal disturbance by free micelles. The ratio c/m, where c is the concentration of detergent not bound to the protein at the CSC (see Section 4.3) and m is the aggregation number, may serve to estimate an upper bound for the micelle concentration in the CSC slot. The fact that c is small for large x suggests that the problem of free micelles may be circumvented by the use of detergents with longer alkyl chains.

5. Conclusions

We have shown that not only detergents determine the solubility of membrane proteins and their properties in aqueous solution, but that *vice versa* the membrane protein affects the aggregation behavior of the detergent. The latter effect not only depends on the binding of detergent to the hydrophobic protein surface, but is probably due to a more general influence of the protein on the free energy of detergent assembly. The critical concentration for both protein solubilisation and detergent aggregation is the CSC, which depends on the protein concentration and can be measured by steady-state fluorescence techniques analogous to the CMC. The dependence of the CSC on the protein concentration is characterised by the constant n_0 (or $\tilde{n}_0$), but n_0 should not be interpreted as the number of detergent molecules bound to the hydrophobic protein surface. Knowledge about the dependence of this constant on the concentration of precipitating agents might be useful to optimise membrane protein crystallisation, e.g., PSIIcc.

Acknowledgements

We thank D. DiFiore for performing titrations, C. Lüneberg for help with protein preparations, Dr. E. Schlodder for allowing us to use his spectrometers, and Prof. R. J. Hunter for sending us supplementary material to his book (FCS). This work was supported by DFG (Sfb 498).

References

[1] D.R. Ort, C.F. Yocum (Eds.), Oxygenic Photosynthesis: The light reactions, Kluwer, Dordrecht, 1996.
[2] J.H. Golbeck (Ed.), Photosystem I, The light-driven plastocyanin:ferredoxin oxidoreductase, Springer, Dordrecht, 2006.
[3] P. Jordan, P. Fromme, H.T. Witt, O. Klukas, W. Saenger, N. Krauss, Three-dimensional structure of cyanobacterial photosystem I at 2.5 Å resolution, Nature 411 (2001) 909–917.
[4] A. Helenius, K. Simons, Solubilization of membranes by detergents, Biochim. Biophys. Acta 415 (1975) 29–79.
[5] R.M. Garavito, S. Ferguson-Miller, Detergents as tools in membrane biochemistry, J. Biol. Chem. 276 (2001) 32403–32406.
[6] P. Rosevear, T. VanAken, J. Baxter, S. Ferguson-Miller, Alkyl glycoside detergents: a simpler synthesis and their effects on kinetic and physical properties of cytochrome *c* oxidase, Biochemistry 19 (1980) 4108–4115.

[7] H. Wennerström, B. Lindman, Micelles. Physical chemistry of surfactant association, Phys. Rep. 52 (1979) 1–86.
[8] D.F. Evans, H. Wennerström, The colloidal domain — where physics, chemistry, and biology meet, Wiley-VCH, New York 1999.
[9] R.J. Hunter, Foundations of colloid science, Oxford University Press, 2001.
[10] K. Holmberg, B. Jönsson, B. Kronberg, B. Lindman, Surfactants and polymers in aqueous solution, Wiley 2003.
[11] F.M. Menger, On the structure of micelles, Acc. Chem. Res. 12 (1979) 111–117.
[12] M. Roth, A. Lewit-Bentley, H. Michel, J. Deisenhofer, R. Huber, D. Oesterhelt, Detergent structure in crystals of a bacterial photosynthetic reaction centre, Nature 340 (1989) 659–662.
[13] M. Roth, B. Arnoux, A. Ducruix, F. Reiss-Husson, Structure of the detergent phase and protein–detergent interactions in crystals of the wild-type (strain Y) *Rhodobacter sphaeroides* photochemical reaction center, Biochemistry 30 (1991) 9403–9413.
[14] P. Timmins, E. Pebay-Peyroula, W. Welte, Detergent organisation in solutions and in crystals of membrane proteins, Biophys. Chem. 53 (1994) 27–36.
[15] E. Pebay-Peyroula, R.M. Garavito, J.P. Rosenbusch, M. Zulauf, P.A. Timmins, Detergent structure in tetragonal crystals of OmpF porin, Structure 3 (1995) 1051–1059.
[16] S.M. Prince, T.D. Howard, D.A.A. Myles, C. Wilkinson, M.Z. Papiz, A.A. Freer, R.J. Cogdell, N.W. Isaacs, Detergent structure in crystals of the integral membrane light-harvesting complex LH2 from *Rhodopseudomonas acidophila* strain 10050, J. Mol. Biol. 326 (2003) 307–315.
[17] M. Ceccarelli, M. Marchi, Simulation and modeling of the *Rhodobacter sphaeroides* bacterial reaction center: Structure and interactions, J. Phys. Chem. B 107 (2003) 1423–1431.
[18] T.L. Hill, An introduction to statistical thermodynamics, Addison-Wesley 1960, Dover edition 1986.
[19] A. George, W.W. Wilson, Predicting protein crystallization from a dilute solution property, Acta Cryst. D 50 (1994) 361–365.
[20] Y. Georgalis, A. Zouni, W. Eberstein, W. Saenger, Formation dynamics of protein precrystallization fractal clusters, J. Crystal Growth 126 (1993) 245–260.
[21] P. Thiyagarajan, D.M. Tiede, Detergent micelle structure and micelle–micelle interactions determined by small-angle neutron scattering under solution conditions used for membrane protein crystallization, J. Phys. Chem. 98 (1994) 10343–10351.
[22] P.A. Marone, P. Thiyagarajan, A.M. Wagner, D.M. Tiede, The association state of a detergent-solubilized membrane protein measured during crystal nucleation and growth by small-angle neutron scattering, J. Crystal Growth 191 (1998) 811–819.
[23] T. Wydrzynski, K. Satoh (Eds.), Photosystem II: The light-driven water:plastoquinone oxidoreductase, Springer, Dordrecht, The Netherlands (2005).
[24] J. Kern, G. Renger, Photosystem II: Structure and mechanism of the water: plastoquinone oxidoreductase, Photosynth. Res. 94 (2007) 183–202.
[25] A. Zouni, J. Kern, J. Frank, T. Hellweg, J. Behlke, W. Saenger, K.D. Irrgang, Size determination of cyanobacterial and higher plant photosystem II by gel permeation chromatography, light scattering and ultracentrifugation, Biochemistry 44 (2005) 4572–4581.
[26] P.A. Marone, P. Thiyagarajan, A.M. Wagner, D.M. Tiede, Effect of detergent alkyl chain length on crystallization of a detergent-solubilized membrane protein: correlation of protein–detergent particle size and particle–particle interaction with crystallization of the photosynthetic reaction center from *Rhodobacter sphaeroides*, J. Crystal Growth 207 (1999) 214–225.
[27] K. Kalyanasundaram, J.K. Thomas, Environmental effects on vibronic band intensities in pyrene monomer fluorescence and their application in studies of micellar systems, J. Am. Chem. Soc. 99 (1977) 2039–2044.
[28] C.J. Drummond, G.G. Warr, F. Griesner, B.W. Ninham, D.F. Evans, Surface properties and micellar interfacial microenvironment of *n*-dodecyl β-D-maltoside, J. Phys. Chem. 89 (1985) 2103–2109.
[29] M. Aoudia, R. Zana, Aggregation behavior of sugar surfactants in aqueous solutions: Effects of temperature and the addition of nonionic polymers, J. Colloid Interface Sci. 206 (1998) 158–167.
[30] L. Sahoo, J. Sarangi, P.K. Misra, Organization of amphiphiles, part 1: Evidence in favor of pre-micellar aggregates through fluorescence spectroscopy, Bull. Chem. Soc. Jpn. 75 (2002) 859–865.
[31] G.B. Ray, I. Chakraborty, S.P. Moulik, Pyrene absorption can be a convenient method for probing critical micellar concentration (cmc) and indexing micellar polarity, J. Colloid Interface Sci. 294 (2006) 248–254.
[32] T. Sakai, Y. Kaneko, K. Tsujii, Premicellar aggregation of fatty acid *N*-methylethanolamides in aqueous solutions, Langmuir 22 (2006) 2039–2044.
[33] J.N. Israelachvili, D.J. Mitchell, B.W. Ninham, Theory of self-assembly of hydrocarbon amphiphiles into micelles and bilayers, J. Chem. Soc., Faraday Trans. 2 (72) (1976) 1525–1568.
[34] S. Puvvada, D. Blankschtein, Molecular-thermodynamic approach to predict micellization, phase behavior and phase separation of micellar solutions: I. Application to nonionic surfactants, J. Chem. Phys. 92 (1990) 3710–3724.
[35] R. Nagarajan, E. Ruckenstein, Theory of surfactant self-assembly: a predictive molecular thermodynamic approach, Langmuir 7 (1991) 2934–2969.
[36] P. Gast, P. Hemelrijk, A.J. Hoff, Determination of the number of detergent molecules associated with the reaction center protein isolated from the photosynthetic bacterium *Rhodopseudomonas viridis*. Effects of the amphiphilic molecule 1,2,3-heptanetriol, FEBS Lett. 337 (1994) 39–42.
[37] P. Gast, P.W. Hemelrijk, H.J. Van Gorkom, A.J. Hoff, The association of different detergents with the photosynthetic reaction center protein of *Rhodobacter sphaeroides* R26 and the effects on its photochemistry, Eur. J. Biochem. 239 (1996) 805–809.
[38] F. Müh, J. Rautter, W. Lubitz, Effects of zwitterionic detergents on the primary donor of bacterial reaction centers, Ber. Bunsenges. Phys. Chem. 100 (1996) 1974–1977.
[39] F. Müh, A. Zouni, Extinction coefficients and critical solubilisation concentrations of photosystems I and II from *Thermosynechococcus elongatus*, Biochim. Biophys. Acta 1708 (2005) 219–228.
[40] W. Saenger, A. Müller-Fahrnow, Cyclodextrins increase surface tension and critical micelle concentrations of detergent solutions, Angew. Chem. Int. Ed. Engl. 27 (1988) 393–394.
[41] W.J. De Grip, J. Van Oostrum, P.H.M. Bovee-Geurts, Selective detergent-extraction from mixed detergent/lipid/protein micelles, using cyclodextrin inclusion compounds: a novel generic approach for the preparation of proteoliposomes, Biochem. J. 330 (1998) 667–674.
[42] G.A. Signorell, T.C. Kaufmann, W. Kukulski, A. Engel, H.W. Rémigy, Controlled 2D crystallization of membrane proteins using methyl-β-cyclodextrin, J. Struct. Biol. 157 (2007) 321–328.
[43] B. Vulliez-Le Normand, J.L. Eiselé, Determination of detergent critical micellar concentration by solubilization of a colored dye, Anal. Biochem. 208 (1993) 241–243.
[44] R. Nechushtai, S.D. Nourizadeh, J.P. Thornber, A reevaluation of the fluorescence of the core chlorophylls of photosystem I, Biochim. Biophys. Acta 848 (1986) 193–200.
[45] R. Croce, G. Zucchelli, F.M. Garlaschi, R. Bassi, R.C. Jennings, Excited state equilibrium in the photosystem I-light-harvesting I complex: P700 is almost isoenergetic with its antenna, Biochemistry 35 (1996) 8572–8579.
[46] L.O. Pålsson, C. Flemming, B. Gobets, R. van Grondelle, J.P. Dekker, E. Schlodder, Energy transfer and charge separation in photosystem I: P700 oxidation upon selective excitation of the long-wavelength antenna chlorophylls of *Synechococcus elongatus*, Biophys. J. 74 (1998) 2611–2622.
[47] M. Byrdin, Messungen und Modellierungen zur Dynamik angeregter Zustände in Photosystem I, PhD thesis, Free University of Berlin, 1999.
[48] P. Jekow, P. Fromme, H.T. Witt, W. Saenger, Photosystem I from *Synechococcus elongatus*: preparation and crystallization of monomers with varying subunit composition, Biochim. Biophys. Acta 1229 (1995) 115–120.
[49] P. Fromme, H.T. Witt, Improved isolation and crystallization of photosystem I for structural analysis, Biochim. Biophys. Acta 1365 (1998) 175–184.
[50] J. Kern, B. Loll, C. Lüneberg, D. DiFiore, J. Biesiadka, K.D. Irrgang, A. Zouni, Purification, characterisation and crystallisation of photosystem II from *Thermosynechococcus elongatus* cultivated in a new type of photobioreactor, Biochim. Biophys. Acta 1706 (2005) 147–157.
[51] H. Zettl, Y. Portnoy, M. Gottlieb, G. Krausch, Investigation of micelle formation by fluorescence correlation spectroscopy, J. Phys. Chem. B 109 (2005) 13397–13401.
[52] H. O'Neill, W.T. Heller, K.E. Helton, V.S. Urban, E. Greenbaum, Small-angle X-ray scattering study of photosystem I-detergent complexes: implications for membrane protein crystallization, J. Phys. Chem. B 111 (2007) 4211–4219.
[53] S. Wang, S. Lin, X. Lin, N.W. Woodbury, J.P. Allen, Comparative study of reaction centers from purple photosynthetic bacteria: isolation and optical spectroscopy, Photosynth. Res. 42 (1994) 203–215.
[54] J. Rautter, F. Lendzian, W. Lubitz, S. Wang, J.P. Allen, Comparative study of reaction centers from photosynthetic purple bacteria: electron paramagnetic resonance and electron nuclear double resonance spectroscopy, Biochemistry 33 (1994) 12077–12084.
[55] F. Müh, J. Rautter, W. Lubitz, Two distinct conformations of the primary electron donor in reaction centers from *Rhodobacter sphaeroides* revealed by ENDOR/TRIPLE-spectroscopy, Biochemistry 36 (1997) 4155–4162.
[56] F. Müh, C. Schulz, E. Schlodder, M.R. Jones, J. Rautter, M. Kuhn, W. Lubitz, Effects of zwitterionic detergents on the electronic structure of the primary donor and the charge recombination kinetics of $P^+Q_A^-$ in native and mutant reaction centers from *Rhodobacter sphaeroides*, Photosynth. Res. 55 (1998) 199–205.
[57] J.E. Eastman, A.K.W. Taguchi, S. Lin, J.A. Jackson, N.W. Woodbury, Characterization of a *Rhodobacter capsulatus* reaction center mutant that enhances the distinction between spectral forms of the initial electron donor, Biochemistry 39 (2000) 14787–14798.
[58] C. Kirmaier, P.D. Laible, E. Hindin, D.K. Hanson, D. Holten, Detergent effects on primary charge separation in wild-type and mutant *Rhodobacter capsulatus* reaction centers, Chem. Phys. 294 (2003) 305–318.
[59] G. Palazzo, A. Mallardi, F. Francia, M. Dezi, G. Venturoli, M. Pierno, E. Vignati, R. Piazza, Spontaneous emulsification of detergent solubilized reaction center: protein conformational changes precede droplet growth, Phys. Chem. Chem. Phys. 6 (2004) 1439–1445.
[60] S. Bogusz, R.M. Venable, R.W. Pastor, Molecular dynamics simulations of octyl glucoside micelles: structural properties, J. Phys. Chem. B 104 (2000) 5462–5470.
[61] S. Wolfram, The Mathematica book, 4th ed., Wolfram Media/Cambridge University Press, 1999.
[62] A. Sen, W.P. Williams, P.J. Quinn, The structure and thermotropic properties of pure 1,2-digalactosylglycerols in aqueous systems, Biochim. Biophys. Acta 663 (1981) 380–389.
[63] C. Cecutti, B. Focher, B. Perly, T. Zemb, Glycolipid self-assembly: micellar structure, Langmuir 7 (1991) 2580–2585.
[64] I. Simidjiev, S. Stoylova, H. Amenitsch, T. Jávorfi, L. Mustárdy, P. Laggner, A. Holzenburg, G. Garab, Self-assembly of large, ordered lamellae from non-bilayer lipids and integral membrane proteins *in vitro*, Proc. Natl. Acad. Sci. U.S.A. 97 (2000) 1473–1476.
[65] L. Bamber, M. Harding, P.J.G. Butler, E.R.S. Kunji, Yeast mitochondrial ADP/ATP carriers are monomeric in detergents, Proc. Natl. Acad. Sci. U.S.A. 103 (2006) 16224–16229.

[66] K. Lum, D. Chandler, J.D. Weeks, Hydrophobicity at small and large length scales, J. Phys. Chem. B 103 (1999) 4570–4577.
[67] D. Chandler, Two faces of water, Nature 417 (2002) 491.
[68] P. Ball, How to keep dry in water, Nature 423 (2003) 25–26.
[69] D. Chandler, Interfaces and the driving force of hydrophobic assembly, Nature 437 (2005) 640–647.
[70] P. Ball, Water as an active constituent in cell biology, Chem. Rev. 108 (2008) 74–108.
[71] A. Zouni, H.T. Witt, J. Kern, P. Fromme, N. Krauss, W. Saenger, P. Orth, Crystal structure of photosystem II from *Synechococcus elongatus* at 3.8 Å resolution, Nature 409 (2001) 739–743.
[72] B. Loll, J. Kern, W. Saenger, A. Zouni, J. Biesiadka, Towards complete cofactor arrangement in the 3.0 Å resolution structure of photosystem II, Nature 438 (2005) 1040–1044.
[73] A. Zouni, From cell growth to the 3.0 Å resolution crystal structure of cyanobacterial photosystem II, in: G. Renger (Ed.), Primary Processes of Photosynthesis, Principles and Apparatus, Part 2, Royal Society Chemistry Publishing, Cambridge, 2008.
[74] D. Danino, Y. Talmon, R. Zana, Aggregation and microstructure in aqueous solutions of the nonionic surfactant $C_{12}E_8$, J. Colloid Interface Sci. 186 (1997) 170–179.
[75] J. Lipfert, L. Columbus, V.B. Chu, S.A. Lesley, S. Doniach, Size and shape of detergent micelles determined by small-angle X-ray scattering, J. Phys. Chem. B 111 (2007) 12427–12438.